Sov. Lightwave Commun. 3 (1993) 77–86. Printed in the UK

# Soliton propagation and polarization mode-locking in birefringent optical fibres

V V Afanasjev and A B Grudinin

Russian Academy of Sciences, General Physics Institute, Vavilova Street 38, Moscow 117942, Russia

Received 31 July 1992, in final form 5 May 1993

**Abstract.** Soliton propagation in polarization-preserving fibres is analysed. Based on the coupled nonlinear Schrödinger equations we derive an analytical approximation for such type of soliton propagation. Exploitation of soliton polarization properties for passive mode-locking in fibre lasers is also considered.

## 1. Introduction

In recent years much work has been devoted to the development of erbium-doped fibre lasers [1–9], because a broad gain bandwidth centred nearly 1.54 $\mu$m, negative group velocity dispersion and tight confinement of optical field allow the exploitation of nonlinear optical effects for very efficient generation of ultra-short optical pulses.

In the last few years several schemes of fibre soliton lasers have been reported [2–9]. Experimental study of such lasers has revealed a strong influence of fibre birefringence on laser output characteristics.

Polarization properties of optical fibres manifest themselves more clearly in mode-locked systems based on polarization switch [7–9]. It is interesting that the desirable effect can be reached in both linear [7] and ring configurations [8, 9].

Thus the problem of soliton propagation in birefringent optical fibres becomes of considerable interest and various aspects of the problem have been studied in many papers [10–15].

As has been shown [10–12] a bound state of orthogonally polarized solitons can exist in fibres with arbitrary birefringence provided there is compensation of polarization time delay by the group velocity dispersion that causes spectral separation of orthogonal components. Formally it means that, if input conditions for the coupled nonlinear Shrödinger equations have a properly designed spectrum, the term describing birefringence can be omitted.

Another soliton behaviour occurs if an initial pulse has unshifted spectral components. In this case there will be a transient region, characterized by an oscillating behaviour of the orthogonal spectral components and depending upon the value of birefringence this process might result in formation either of a single soliton with coupled polarization components or two independent solitons with an orthogonal state of polarization.

Thus the problem of soliton propagation in an optical fibre has in fact two aspects.

The first question is concerned with polarization evolution of the steady bound state of orthogonally polarized solitons. This problem is closely related to an effect of polarization intensity discrimination which plays a key role in the operational principle of a passive mode-locked laser based on polarization switch [8, 9], and in the general case this problem

0960-0884/93/020077+10$07.50 © 1993 IOP Publishing Ltd 

has not yet been solved. Manassah [16] and Malomed and Wabnitz [17] have considered a case when one polarization component is much smaller than the other one. But the practically interesting case for passive mode-locking when the polarization component ratio is around 2 has so far no solution.

The second aspect is related to soliton formation from low level noise in an fibre amplifier which, in particular, takes place in fibre lasers. In this instance fibre birefringence plays a significant role and affects the capability of the laser to pass into self-started mode-locking.

Taking into consideration the importance of fibre polarization properties for fibre laser performance we consider in this paper soliton propagation along a birefringent fibre and show how intensity dependent birefringence causes passive mode-locking. We also discuss the influence of various fibre laser parameters on the quality of mode-locked pulses.

## 2. Soliton propagation in birefringent fibres

### 2.1. Analytical approach

We begin our consideration from the system of coupled nonlinear Schrödinger equations in the form [18]

$$\begin{aligned} i\left(\frac{\partial\psi_1}{\partial z}+\delta\frac{\partial\psi_1}{\partial\tau}\right)+\frac{1}{2}\frac{\partial^2\psi_1}{\partial\tau^2}+(|\psi_1|^2+\gamma|\psi_2|^2)\psi_1=0 \\ i\left(\frac{\partial\psi_2}{\partial z}-\delta\frac{\partial\psi_2}{\partial\tau}\right)+\frac{1}{2}\frac{\partial^2\psi_2}{\partial\tau^2}+(|\psi_2|^2+\gamma|\psi_1|^2)\psi_2=0 \end{aligned} \tag{1}$$

where $\gamma = 2$ for circularly polarized eigenmodes $\psi_1$ and $\psi_2$ and $\gamma = 2/3$ for linearly polarized ones. $\delta = B\tau_0/(2|k''|)$ and $B$ is a fibre birefringence.

Since we consider here a steady bound state, then $\delta = 0$. These equations have the well-known exact soliton solution

$$\psi_i(\tau, z) = A_i \operatorname{sech}(\tau)\exp(-i\Gamma_i z) \qquad i = 1, 2, \tag{2}$$

where $A_i$, $\Gamma_i$ are some constants, and the relationship between $A_i$, $\Gamma_i$ may be found by direct substitution of (2) to (1). However, solution (2) exists only in three particular cases: (i) Manakov's case, when $\gamma = 1$, (ii) only one polarization is excited $A_1 = 1$, $A_2 = 0$, or vice versa, (iii) the symmetric case $A_1 = A_2 = 1/\sqrt{1+\gamma}$.

We seek an approximate solution in the form (2), where now $A_i$ and $\Gamma_i$ are functions of the polarization angle $\alpha$. Let us introduce the unknown real soliton amplitude $\rho(\alpha)$, then $A_1 = \rho(\alpha)\cos\alpha$, $A_2 = \rho(\alpha)\sin\alpha$. The function $\rho(\alpha)$ should satisfy the boundary conditions $\rho(0) = \rho(\pi/2) = 1$, $\rho^2(\pi/4) = 2/(1+\gamma)$ and should be periodical with period $\pi/2$. To find this function in an explicit form, we substitute (2) into (1)

$$\cosh^{-3}(\tau)[(\Gamma_i - 1/2 + S_i)\cosh^2\tau + (1 - S_i)\sinh^2\tau]A_i = D_i \tag{3}$$

where $S_i = A_i^2 + \gamma A_{3-i}^2$, and $D_i = D_i(\tau)$ are the discrepancies. These discrepancies arise in the right-hand side of (1) because we use the approximation (2) instead of exact solution, and we suppose that $|D_i|$ do not depend on $z$. We assume that $\Gamma_i$ should satisfy the relationships

$$\Gamma_i = 1/2 - S_i \tag{4}$$

so

$$D_i = (1 - S_i)A_i \sinh^2(\tau)\cosh^{-3}(\tau). \tag{5}$$

After integration (5) from $-\infty$ to $+\infty$ on $\tau$ we obtain

$$T_1^2 + T_2^2 = \rho^2[(S_1 - 1)^2\cos^2(\alpha) + (S_2 - 1)^2\sin^2(\alpha)]. \tag{6}$$

where

$$T_i = \int D_i(\tau)\,d\tau\left(\int \sinh^2(\tau)\cosh^{-3}(\tau)\,d\tau\right)^{-1}. \tag{7}$$

After integration (6) from 0 to $\pi/2$ on $\alpha$ we obtain a functional of unknown function $\rho(\alpha)$

$$J(\rho) = \int_0^{\pi/2}[T_1^2(\rho) + T_2^2(\rho)]\,d\alpha. \tag{8}$$

To find $\rho(\alpha)$ the functional $J$ should be minimized. Because the sub-integral expression does not depend on the derivative of $\rho(\alpha)$, the Euler–Lagrange condition of functional minimum means:

$$d(T_1^2 + T_2^2)/d\rho = 0. \tag{9}$$

After substitution (6) in (9) we obtain

$$d(T_1^2 + T_2^2)/d\rho = 2\rho(3A\rho^4 + 2B\rho^2 + C) \tag{10}$$

where

$$A = \cos^5\alpha + \sin^6\alpha + (2\gamma + \gamma^2)\sin^2\alpha\cos^2\alpha$$

$$B = -2(\cos^4\alpha + 2\gamma\cos^2\alpha\sin^2\alpha + \sin^4\alpha) \qquad C = 1. \tag{11}$$

Introducing $r = \rho^2$, we obtain a square equation with respect to $r$. The first root of this equation (corresponding to '+') is the solution we are looking for

$$\rho^2(\alpha) = r_1 = (-B + \sqrt{B^2 - 3AC})/3A. \tag{12}$$

Figure 1 shows the graphic representation of this function and the insert represents the discrepancy at $\gamma = 2/3$.

### 2.2. *Numerical results and discussion*

To examine the accuracy of analytical solution (12) we have numerically solved the system (1). The system (1) has been solved by the usual split-step method with a Fast Fourier Transform at the dispersion step and (2) and (12) as initial conditions. The propagation distance has been chosen as long as 40 dispersion lengths to ensure a steady state regime of soliton travelling.

Numerical solution of the system (1) shows that the variation between analytical and numerical solutions are small enough (figure 1). The computer simulation has also shown

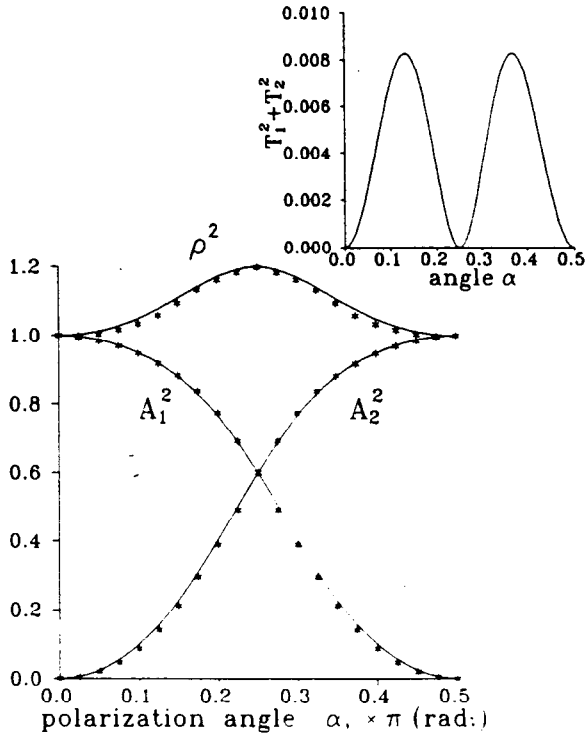


**Figure 1.** Dependences of full soliton intensity $\rho^2$ and intensities of $x$ and $y$ polarization components $A_1^2$ and $A_2^2$ on polarization angle $\alpha$; lines are analytical approximation (12), asterisks—numerical calculations. Insert shows the sum of discrepancies.

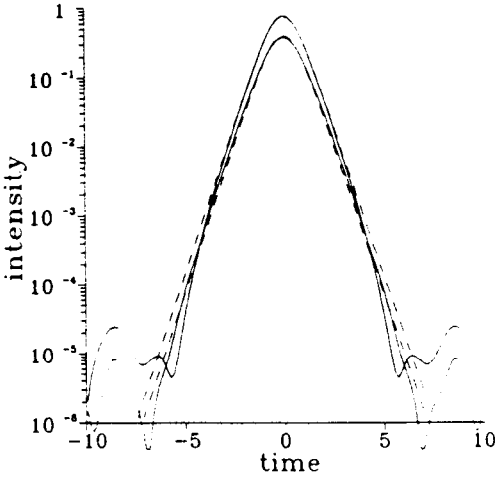


**Figure 2.** Numerical simulation of two-component soliton propagation: the intensities of polarization components at the input (dashed lines) and at $z = 40$ (solid lines).

that both the approximate solution (2) and the representation of the function by (12) have marginally small deviation from the numerical results.

Propagation over 40 dispersion lengths causes small changes (less than 1%) in the soliton amplitude accompanied by insignificant growth of smaller soliton pulsewidth (figure 2).

The pedestal formation may be explained by the fact that the initial nonlinear pulse is not an exact solution of (1) and therefore the originally 'ragged' soliton throws off the

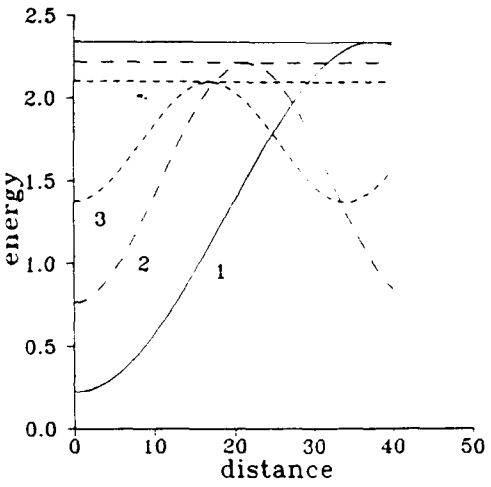


**Figure 3.** Polarization intensity discrimination: dependences of energy after polarizer on propagation distance for $\alpha = 0.2\pi$ (1), $\alpha = 0.15\pi$ (2) and $\alpha = 0.1\pi$ (3). Upper lines are the energies before polarizer.

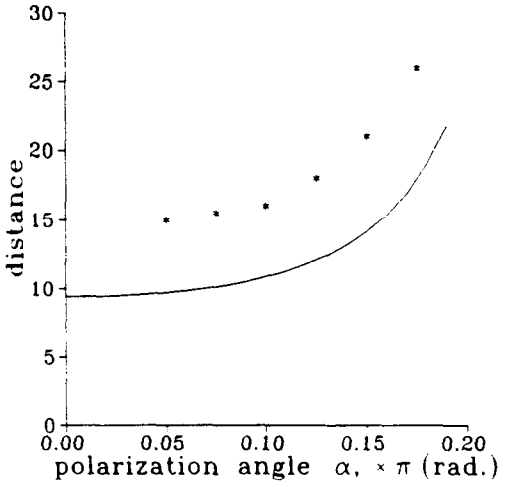


**Figure 4.** Dependence of fibre length of optimal polarization switch on polarization angle $\alpha$, theoretical curve (13) and numerical calculations (asterisks).

dispersive wave which is an origin of the pedestal.

We would like to point out the increase of soliton amplitude with its azimuth with respect to the fibre axis (see figure 1), which may indicate an increase of the soliton energy for constant pulsewidth or decreasing pulsewidth for a given energy. The former case is likely to take place in the figure 8 laser, having a constant pulsewidth defined by the length and dispersion of the laser cavity. Small variation in the state of polarization of the circulating pulses originating from their fluctuation nature results in its different energy, which has been observed experimentally [19].

Evolution of the soliton state of polarization has one very important application i.e. the possibility of exploiting this effect for polarization mode-locking (PML).

The basic idea of PML is different loss for linear and nonlinear waves provided by a polarizer placed and oriented in the proper position. To consider how a soliton passes a polarizer let us look at the nonlinear phase difference between two orthogonal components.

In deriving (12), we have assumed that the phases of these two components obey the relations (4) and the distance at which an effective polarization discrimination occurs might be defined as

$$L = \pi/(S_1 - S_2) \tag{13}$$

i.e. at this distance the phase difference of the two components is equal to $\pi$.

Since the relation (13) is based on an approximate solution of the system (1), we have checked this result in computer simulations. A polarizer has been modelled as

$$\hat{P} = \begin{pmatrix} \cos\alpha & \sin\alpha \\ -\sin\alpha & \cos\alpha \end{pmatrix} \begin{pmatrix} 1 & 0 \\ 0 & 0 \end{pmatrix} \begin{pmatrix} \cos\alpha & -\sin\alpha \\ \sin\alpha & \cos\alpha \end{pmatrix} \tag{14}$$

Figure 3 shows the result of polarization discrimination (energies before and after the polarizer) depending upon normalized fibre length. Note that for any input azimuth $\alpha$ the maximum transmission exceeds 99%, which indicates the bandwidth-limited nature of the passing pulses.

Figure 4 represents the dependence of the fibre length corresponding to maximum transmission against input polarization azimuth or (that is, equivalently) polarization component ratio. One can see that the analytical and numerical dependencies are in good qualitative agreement in the practically interesting range $\alpha = 0.2\pi$ ($A_1/A_2 = 2$ for $\alpha = 0.194\pi$).

## 3. Polarization mode-locking

### *3.1. Numerical results*

We consider the simplest ring configuration shown schematically in figure 5 which is similar to that described in [9]. It consists of an optical fibre having length $L$, a polarizer, polarization control discs (PC) and an isolator providing unidirectional generation.

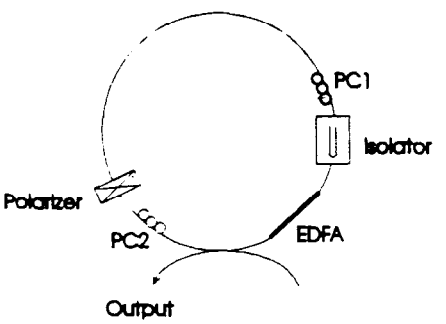


**Figure 5.** Scheme of soliton fibre ring laser with polarization mode locking.

In the steady-state regime the output signal from the right passes the polarizer and relaunches into the fibre from the right exciting both eigenpolarized modes. Both waves then attain differential linear and nonlinear phase delays, establishing under certain conditions a bounded steady state.

As has been shown experimentally [9], an intensity-dependent transmission, and proper position and orientation of the polarizer, results in lower loss for a steady-state soliton in comparison with cw radiation, which in turn leads to a mode-locked regime of the laser. Recently a fibre ring soliton laser has been considered numerically in [20], where dispersionless approximation was used for specification of the soliton polarization. But as has been shown in the previous section, the requisite distance is approximately 20 dispersion lengths and the possibility of using the dispersionless approximation is questionable.

Based on the results from the previous section it is easy to define the position and azimuth of the polarizer and fibre length, required for self-starting of the system. From the results represented in figure 4 one can see that to achieve $\pi$ relative phase difference one needs about 20 dispersion lengths of the steady-state soliton pulses. In physical units it means that for a dispersion $D = 15$ ps nm$^{-1}$ km$^{-1}$ and steady-state pulsewidth of 1 ps the required differential phase shift is achieved at the length of 400 m.

To demonstrate the ability of such configuration to provide a self-started mode-locking regime we have carried out computer simulations of this laser, based on the coupled nonlinear Schrödinger equations (1). We adopt a lumped model of an amplifier described by the following expression

$$\psi_i^{\mathrm{A}}(\omega) = \exp\left(\frac{G}{1+\omega^2\gamma^2}\right)\psi_i(\omega) \tag{15}$$

i.e. we assume a Lorentzian shape of gain with bandwidth equal to $\gamma$ (here $\psi_i(\omega)$ and $\psi_i^A(\omega)$ are normalized fields before and after the amplification, correspondingly).

Laser saturation effects have been taken into account by the expression

$$G = G_0/(1 + E/E_{sat}) \tag{16}$$

where $E$ is the total intracavity energy and $E_{sat}$ is the energy of saturation.

We have performed a set of numerical calculations to reveal key points affecting the performance of this laser.

In the first set we have choose a long, low intensity pulse as an initial signal

$$\psi_1(\tau, z = 0) = \rho(\alpha)\cos(\alpha)\kappa\ \mathrm{sech}(\kappa\tau)$$

$$\psi_2(\tau, z = 0) = \rho(\alpha)\sin(\alpha)\kappa\ \mathrm{sech}(\kappa\tau). \tag{17}$$

This situation takes place when a phase or amplitude modulator is incorporated into the laser cavity. Our results show that the system is able to maintain one or several pulses depending upon saturation intensity (figures 6(*a*)and (*b*)).

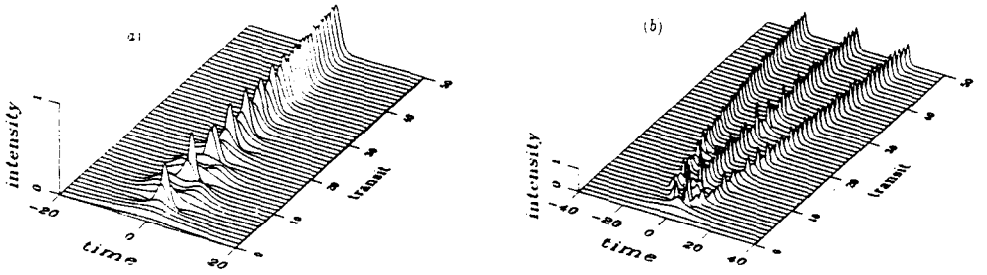


**Figure 6.** Start of laser from weak long pulse (17) to one-pulse (*a*) and three-pulse (*b*) regime. $\kappa = 0.1$; $E_{sat} = 1.25$ and $E_{sat} = 4.5$, correspondingly.

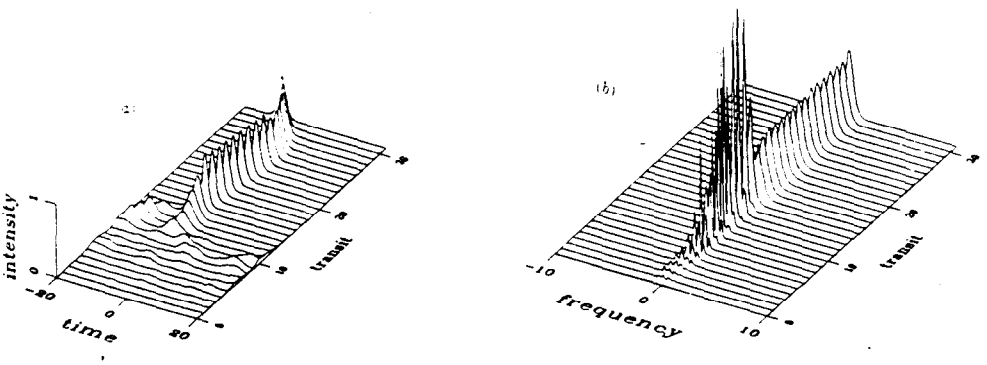


**Figure 7.** Start of laser from noise level: (*a*) intensity, (*b*) spectrum.

The system is also capable of self-starting from a noise level. Figure 7 shows the results of computer simulations when initial conditions are

$$\psi_{1,2} = \kappa\xi_{1,2}(\tau) \tag{18}$$

where $\xi_{1,2}(\tau)$ are two independent values of random function ($0 < \xi < 1$), $\kappa = 0.01$, $E_{sat} = 1.5$, $\gamma = 0.2$.

### 3.2. Discussion

Obviously the main advantage of this configuration of a self-started mode-locked laser, in comparison for instance with the Figure 8 laser, is its simplicity. In principle the same effect might be exploited in a linear configuration that allows us to avoid the use of an isolator and has been demonstrated experimentally [7]. (Note that the authors of [7] did not claim that the laser described in their paper exploits intensity-dependent birefringence effects. However from the description of the laser behaviour the reader can conclude that nonlinear birefringence is responsible for self-sustained mode-locked regime). An important property of this laser is marginally small changes in soliton amplitude while travelling around the cavity. Long cavity length, relatively small gain and an absence of intracavity beam-splitters lead to the generation of clean solitons with a very small amount of non-soliton component, which is especially attractive for soliton transmission lines.

However the 20 dispersion lengths required for attainment of the differential nonlinear phase shift make the ability of the system to self-start rather low. A possible solution to overcome this problem is to increase transmission of the system in the linear regime. But as our computer simulations show this brings about an undesirable growth of the cw component in the steady-state regime, spoiling the quality of the pulses produced, i.e. pulse to cw component energy ratio.

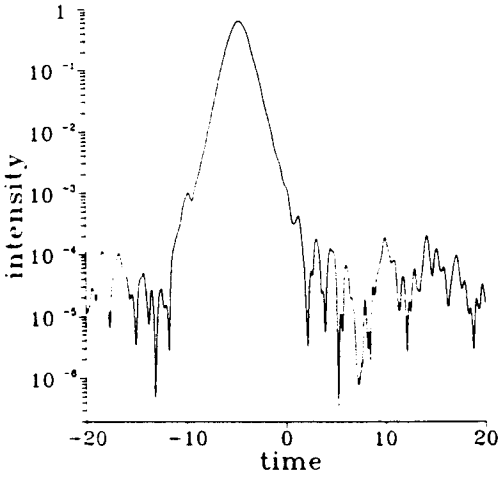


**Figure 8.** Pulse shape in logarithmic scale after start from noise.

Figure 8 shows the shape of the steady pulse on a logarithmic scale for self-starting from noise level. One can see an almost 'ideal' $\mathrm{sech}^2\,\tau$-shape pulse and some pedestal. Note that pedestal intensity is a very important characteristic of any mode-locked laser because it is closely related to peak power of the emitted pulses. However since in a passively mode-locked fibre laser the ratio of round-trip time to pulse duration exceeds $10^3$ then a cw component with intensity $10^{-3}$ less than the soliton intensity substantially modifies the laser output characteristics. The problem of non-soliton component extraction in computer simulations will be considered more fully elsewhere [21].

Our computer simulations also reveal that the system comes into a mode-locked regime not only when the differential phase shift is exactly equal to $\pi$ but also when the cavity length is so short that this value is less than $\pi$ (figure 9) and the residual phase is compensated by the corresponding choice of the PC parameters [22]. However in the last case the pedestal level is higher compared with the pure nonlinear phase shift.

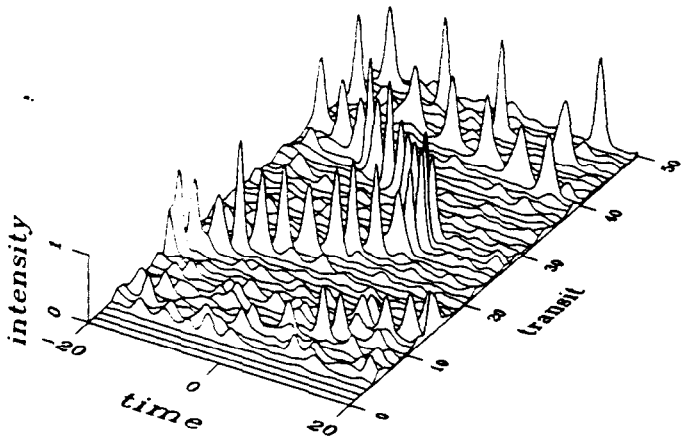


**Figure 9.** Start of laser from noise level for short resonator length $L' = 0.4L$.

This configuration also possesses some features which make it a very promising source for nonlinear transmission lines. In particular, by altering the polarizer azimuth one can easily change the steady-state output pulse duration. Indeed, from (15) one has

$$\tau_s^2(\alpha) \sim L|k''|\cos 2\alpha \tag{19}$$

where $\tau_s(\alpha)$ is steady state pulse width. As azimuth $\alpha$ tends to $\pi/4$, the steady-state pulse duration gets shorter.

Another interesting feature of this laser is the prospect of gradually tuning the operating wavelength by rotating the PCs [9]. It is known [22] that a certain configuration of polarization control discs acts as a $\lambda/2$ plate. Since gain bandwidth of erbium-doped fibres is much broader than a similar value of steady-state laser pulses, it makes it possible to change the operating wavelength by rotating the PCs due to polarization-dependent loss varying periodically with wavelength.

As has been mentioned above, birefringence of an optical fibre causes spectral separation of the polarization components. Therefore we can expect that in the steady-state regime the PML laser output spectrum consists of two peaks and spectral separation between them is defined by the fibre birefringence and group velocity dispersion. For example, for fibre birefringence $B = 10^{-7}$ and chromatic dispersion $D = 15$ ps nm$^{-1}$ km$^{-1}$ the wavelength separation between orthogonal components $\Delta\lambda = 3 \times 10^{-2}$ nm.

An interesting and important question arising out of consideration of PML laser operation is the role of fibre birefringence in the self-starting process. Since for the compensation of polarization dispersion one needs the spectral splitting of the orthogonal components then the PML process can be self-started for any birefringence only if an originally low level seed arising from mode beating has correctly separated spectral components.

On the other hand, one can consider this system as a modification of a laser with fast saturable absorber [23] and operational key points can be described in the framework of the fluctuation model [24]. In the linear stage of the laser output the laser spectrum is (in the absence of any intracavity etalons) a bell-shaped peak at the wavelength of minimal laser loss. Thus, if one does not make any arrangements for dual wavelength generation, the laser starts to operate at a single wavelength and for successful development of a mode-locked pulse one needs to compensate polarization time delay by chromatic

dispersion. Otherwise, if time separation between two polarization components is large enough, then it may destroy the process of PML. For relatively low birefringence one polarization component 'captures' the orthogonal one. This interaction via cross phase modulation results in a bound steady state. Thus, for a successful PML process one needs to use a fibre possessing low birefringence.

The effect of spectral separation has two interesting effects on the laser behaviour. Firstly, in the transient region of steady-state pulse development a variable state of the polarization across the pulse results in some pulse sharpening after passing the polarizer. The second effect is connected with finite gain bandwidth. Since the laser operates at the point of equilibrium gain and loss, then even small spectral separation causes non-uniform gain for orthogonal components that in turn results in a change of polarization state.

## 4. Conclusion

In this paper we have considered soliton propagation in birefringent optical fibres using both an analytical approach and computer simulations. It has been shown that, for a given energy, the soliton pulsewidth depends on the ratio of orthogonal component amplitude.

Based on polarization properties of solitons in birefringent optical fibres we have analysed a passively mode-locked fibre laser, exploiting intensity-dependent birefringence. Such types of lasers have several advantages over other configurations of similar lasers. Beyond the obvious advantage—simplicity—this configuration admits wavelength tuning by the rotation of polarization control discs and pulsewidth tuning by altering the polarizer azimuth.

## References

[1] Digonet M J F 1989 *Soc. Photo-Optical Instrum. Eng. Proc.* **1171**
[2] Kafka J D, Baer T and Hall D W 1989 *Opt. Lett.* **14** 1269
[3] Schlager J B, Yamabayashi Y, Franzen D L and Juineau R I 1989 *IEEE Photon. Technol. Lett.* **1** 264
[4] Smith K, Armitage J R, Wyatt R, Doran N J and Kelly S M J 1990 *Electron. Lett.* **26** 1149
[5] Richardson D J, Laming R I, Payne D N, Matsas V and Phillips M W 1991 *Electron. Lett.* **27** 542
[6] Zirngibl M, Stulz L W, Stone J, Hugi J, DiGiovanni D and Hansen P B 1991 *Electron. Lett.* **27** 1734
[7] Davey R P, Langford N and Ferguson A I 1991 *Electron. Lett.* **27** 1257
[8] Fontana F, Grasso G, Manfredini N, Romagnoli M and Daino B 1992 *Electron. Lett.* **28** 1291
[9] Matsas V J, Newson T P, Richardson D J and Payne D N 1992 *Electron. Lett.* **28** 1391
[10] Menyuk C R 1987 *Opt. Lett.* **12** 614
[11] Menyuk C R 1988 *J. Opt. Soc. Am.* B **5** 392
[12] Islam M N, Poole C D and Gordon J P 1989 *Opt. Lett.* **14** 1011
[13] Vysloukh V A, Kolomiitseva E A and Matveev A N 1991 *Vestnik MGU* **32** 90
[14] Ueda T and Kath W L 1990 *Phys. Rev.* A **42** 563
[15] Afanasjev V V and Serkin V N Interaction of vector solitons in the Manakov model *Opt. Lett.* submitted
[16] Manassah J T 1991 *Opt. Lett.* **16** 587
[17] Malomed B A and Wabnitz S 1991 *Opt. Lett.* **16** 1388
[18] Menyuk C R 1987 *IEEE J. Quantum Electron.* **23** 174
[19] Grudinin A B, Richardson D J and Payne D N 1992 *Electron. Lett.* **28** 59
[20] Chen C-J, Wai P K A and Menyuk C R 1992 *Opt. Lett.* **17** 417
[21] Afanasjev V V and Grudinin A B Numerical study of passively mode-locked soliton fibre laser *IEEE J. Quantum Electron.* submitted
[22] Lefevre H C 1980 *Electron. Lett.* **16** 778
[23] Haus H A, Fujimoto J G and Ippen E P 1991 *J. Opt. Soc. Am.* B **8** 2068
[24] Kryukov P G and Letokhov V S 1972 *IEEE J Quantum Electron.* **8** 766